Laser ultrasonics for non-destructive battery weld evaluation (LUNAR)

Public report

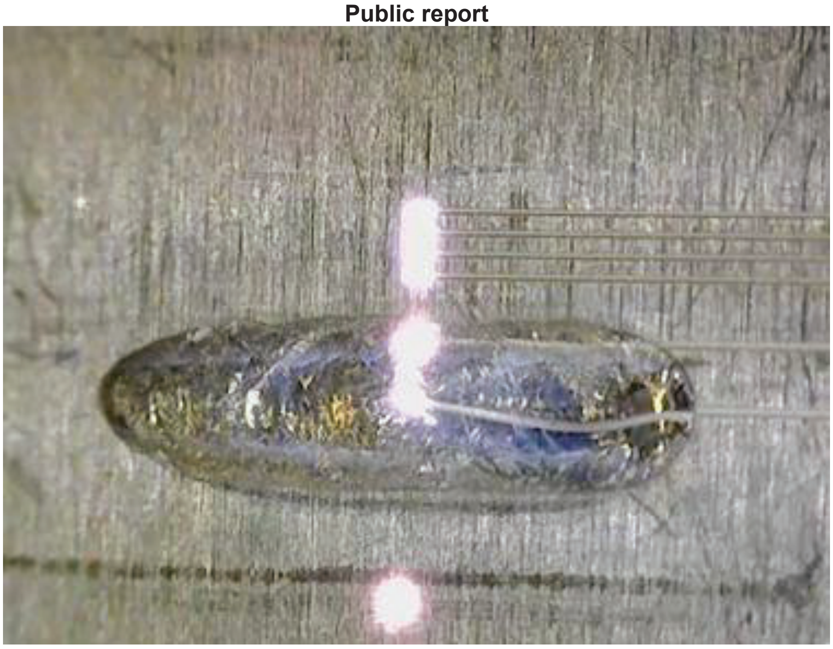

Project within Circularity - FFI - spring 2024

Author Hampus Wikmark Kreuger, Mikael Malmström, Stephanie Robertson, Yves Van den Stock

Date 2025-12-01

FFI Fordonsstrategisk Forskning och Innovation

Content

1. Summary 5

2. Sammanfattning på svenska 5

3. Background 6

4. Purpose, research questions and method 7

4.1 Purpose 7
4.2 Research questions 7
4.3 Methods for LUS measurements 8

5. Objective 10

6. Results and deliverables 11

6.1 Requirements, criteria and evaluation methods in comparison to LUS 11
6.2 Sample selection and take-out 11
6.3 Set-up for evaluation of joints with LUS 12
6.4 LUS measurements and data analysis 13
6.5 Correlation plot showing measured weld area with LUS vs destructive / CT testing.. 20
6.6 Benchmarking LUS with conventional technique 21
6.7 Benchmarking with conventional destructive testing 21
6.8 Measurements with other techniques 23
6.9 Literature study on implementation and benchmarking 23
6.10 A first framework for implementation and requirement specification of hardware and measurement methodology 23
6.11 Set up project website for communication 23
6.12 Technical reports and dissemination 23

7. Dissemination and publications 24

7.1 Dissemination 24
7.2 Publications 24

8. Conclusions and future research 24

8.1 Need for large data sets 24
8.2 Alternate ultrasound geometries 25

9. Participating parties and contact persons 25

10. References 26

FFI in short

FFI, Strategic Vehicle Research and Innovation, is a joint program between the state and the automotive industry running since 2009. FFI promotes and finances research and innovation to sustainable road transport.

For more information: www.ffisweden.se

1. Summary

The LUNAR project has been a pre-study to evaluate laser ultrasonics (LUS) for measurement of battery busbar laser welding. The technique presents a non-contact, nondestructive bulk measurement that only needs access from one side of the sample, potentially enabling in-line measurement of many or all produced batteries. A higher rate of measurement means that faults can be caught quicker, while reducing the required rate of destructive testing leads to a lower rate of material waste and higher production yield.

We have demonstrated the LUS technique on artificial samples with a convincing quantitative correlation between estimated and actual joint width.

Several laser-welded samples have also been measured but with less conclusive results. LUS results on these samples have been qualitatively compared to destructive testing and computed tomography (CT) measurements.

More data is likely needed to find relevant features to correlate with joint characteristics such as depth and width.

2. Sammanfattning på svenska

LUNAR-projektet har utgjort en förstudie för att utvärdera laserultraljud (LUS) som mätmetod för lasersvetsning av strömskenor till fordonsbatterier. Strömskenor är en viktig del av batterierna i elektriska fordon för att fördela strömuttaget jämnt över alla batteriets celler. För att uppnå tillräcklig ledningsförmåga är det dock kritiskt att strömskenan fogas väl mot cellernas terminaler.

I dagsläget finns flera tekniker tillgängliga för att inspektera svetsfogar. Under fogning kan kamerabaserade tekniker och optisk koherent tomografi (OCT) användas, men då de är ljusbaserade beskriver de främst materialets yta. För att undersöka djupare ned i materialet används förstörande provning (då stycket kapas och snittet studeras med mikroskop) eller skiktröntgen-datortomografi (CT). Dessa har dock sina begränsningar; CT kan mäta mindre prover och kan således inte mäta fogen "på plats" i ett större batteri, och förstörande provning innebär förlust av både tid och material.

En möjlig lösning är LUS-tekniken, som är en kontaktlös mätmetod som kan avslöja hur materialet ser ut på djupet. En kort laserpuls skapar vibrationer i ett material, och utbredningen av vibrationerna kan mätas med en annan laser. Defekter eller gränssnitt mellan material ger uppmätbara ekon, som illustreras i figuren nedan. Eftersom både generering och detektion sker med laserstrålar behövs ingen fysisk kontakt, till skillnad mot konventionella ultraljudsmätningar med till exempel piezoelektriska givare.

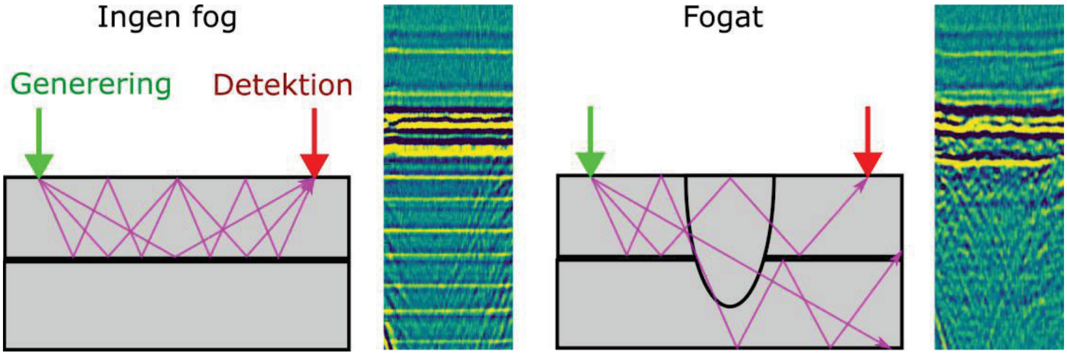

Figur 1: Utbredningen av ultraljudsvågor i ett stycke som inte är fogat till det underliggande materialet, med ett flertal ekon (vänster) och ett som fogats, där flera vågor försvinner genom fogen (höger). De färgglada bilderna visar utdrag ur faktiska mätningar på de två fallen.

I projektet har denna teknik utvärderats dels med hjälp av artificiella svetsar (gnistbearbetade prover) och prover framtagna med produktionsutrustning. I de artificiella proverna kan bredden på "svetsfogen" uppskattas med god noggrannhet. För de svetsade proverna är det svårare att avgöra vilka signaler som överensstämmer med fogens egenskaper (bredd, hålighet, mm.) och vilka som kommer av exempelvis ytdefekter. Några prover har också utvärderats med CT och/eller förstörande provning.

Som slutsats vet vi mer om hur LUS-tekniken skulle kunna användas, men har förstått att mer data, både från LUS-mätningar och från kompletterande tekniker som datortomografi och förstörande provning, förmodligen är nödvändigt för att uppnå en tillräckligt robust mätmetod för batterikvalitet.

3. Background

Electric vehicle (EV) battery production relies on efficient and reliable welding processes to join bus bars, the metal strips that connect individual cells within the battery pack, allowing them to function collectively as a single unit. These bus bars are typically joined by laser welding and are essential components in EV batteries for electrical connectivity, thermal management, and overall performance. The properties and stability of the battery pack depend greatly on how well the bars are joined[1,2]. Faulty joints in one location can lead to increased energy density in others, increasing the risk of unstable behavior, especially thermal runaway and fire.

An industrial challenge to inspection of critical joints, such as the laser welds of busbar tabs in battery manufacturing for electronic vehicles, is the relatively small dimension of the weld compared to the size of the component on which it is found. Component size often dictates the methods by which it can be inspected, though the cost in terms of revenue and waste also influences the preferred inspection methods.
The consumption of resources in the manufacturing of a battery module is sufficient that automotive manufacturers would like to use as much non-destructive testing as possible

for their products. This, however, needs to be balanced with the resource demand of inspecting large components and the safety of the staff to do so.

Traditional methods for measuring the welded area of laser welds in bus bars often involve destructive testing (microscopy) or complex X-ray metrology techniques, which can be time-consuming, expensive, and impractical for high-volume production. One potential solution is laser ultrasonics (LUS).

As a non-contact and nearly instantaneous measurement technique, LUS has already proven useful in other applications, e.g., online microstructure measurement during hot rolling[3,4] or during thermomechanical simulations[5–10] and shown potential for evaluation of weld joint quality[11–16], by itself or in combination with electromagnetic acoustic transducers (EMAT)[17].

Compared to other methods for verifying weld quality such as optical coherence tomography / coherent imaging[18–20] and camera-based methods[21], LUS does not just probe the keyhole or surface, but the generated ultrasound waves travel through the bulk of the material. LUS shares this capability with IR thermography[2,22] but without the drawback of needing access to both sides of the joint, making it more suitable for in-line inspection in the production line. Traditional ultrasound measurements, e.g. by piezoelectric transducers[23], requires contact with the material, which presents hazards to both operators and equipment when measuring on EV batteries due to the risk of electrical discharge, and poses challenges to implementation in an inline setting.

4. Purpose, research questions and method

4.1 Purpose

The purpose of this project is to advance quality assurance practice in EV battery production by exploring the potential of LUS measurements. Improving the quality of battery production is expected to increase the competitiveness of the Swedish automotive industry and to a more sustainable transport sector.

The current industrial standard is to perform destructive testing on components to ensure their quality. This inherently leads to waste as the component cannot be used further for production. However, the information that is gathered is of high importance and value. To ensure process validation while minimizing waste, it is essential to rigorously validate non-destructive testing methods with high-quality standards. By doing so, the reliance on destructive testing can be reduced, allowing for longer intervals between destructive tests and supporting continuous quality assurance through robust non-destructive observations.

4.2 Research questions

The research questions asked in this project can be expressed as follows:

- What are the possibilities and limitations for the use of LUS technology in battery manufacturing?

- How far is the state of the art in measurement from the ideal case of in-line quantitative non-destructive testing in bulk, and how can this be achieved?
- What techniques and/or methods (destructive testing, CT, and others) could possibly be replaced by LUS, and which are complementary?

4.3 Methods for LUS measurements

As a first measure of a weld, it is possible to study the reflection of ultrasonic waves in the interface between two pieces[15]. This is because there is typically a reflection in this interface, but a weld may disrupt the reflections by transmission or diffraction. An example of this is shown in Figure 2 below, with the ultrasonic waves generated with one laser pulse (green arrow) and the response on the other side of the weld is measured by another laser beam (red arrow). In the figure a typical B-scan of a scan along the length of a weld is also displayed next to the illustrations showing the different echoes as dark and bright yellow horizontal lines. For the no weld measurement, the ultrasound reverberates back and forth in the material for a long time, whereas in the measurement of a weld the ultrasound is attenuated and scattered resulting in the later echoes missing (bright yellow lines in the bottom half of the B-scan).

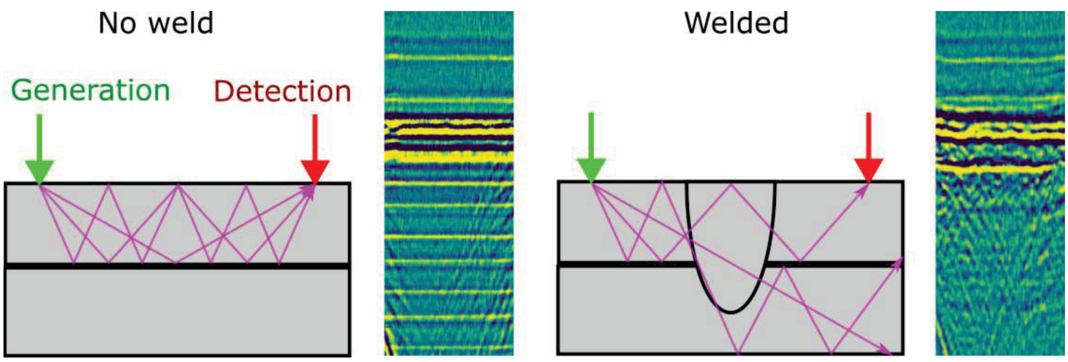

Figure 2: The propagation of ultrasonic waves and reflection at an interface between two metal pieces (left) and several lost reflections when the two pieces have been welded together (right). The graphic inserts show actual LUS B-scans on uncoupled and welded sections, respectively. The X-direction indicate the position on the sample, whereas the Y-direction represents the time in the measurement after the ultrasonic generation.

To assess the potential for LUS measurements to improve quality control for welded battery bus bars, several campaigns of LUS measurements were performed in Swerim’s laboratory. The measurements followed two principal directions:

1. **Measurements on electric discharge machining (EDM) manufactured pieces** with known / designed features mimicking those of welded workpieces.
2. **Measurements on welded pieces** manufactured by the participating companies, using actual production parameters or with an exaggerated range of parameters to create measurable defects.

The results in these two directions are described in detail in section 6.4.

Two LUS measurement systems were used in the described experiments, referred to here as the high-power (HP) and high-frequency (HF) systems. The designs of the systems, along with some key parameters, are shown below.

The HP system features a detection laser system consisting of a Tecnar PDL 1064 nm laser and Tecnar TWM receiver, along with a frequency doubled Quantel pulsed laser with 532 nm wavelength for generation.

Figure 3: Photos of (left) the detection laser system, and (right) the generation laser system of the high power (HP) measurement system.

The HF system uses an Azurlight 1030 nm fiber laser and Tecnar TWM receiver for detection and an IPG Photonics 1064 nm wavelength laser for generation.

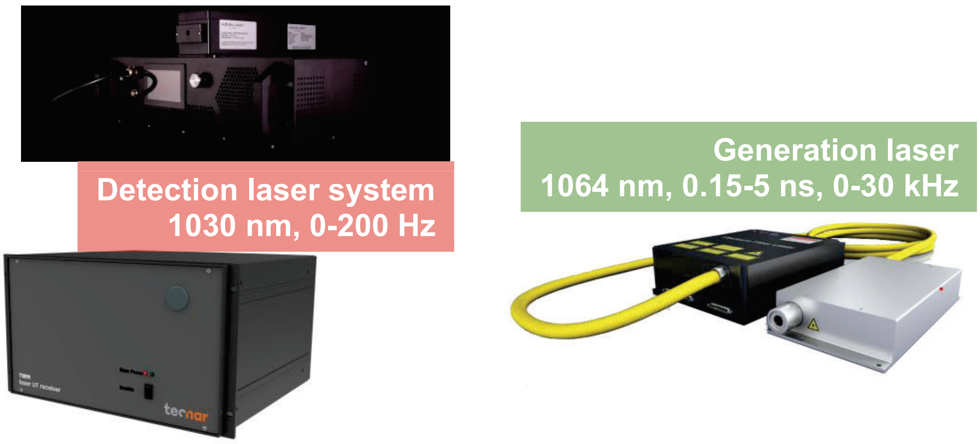

Figure 4: Photos of (left) the detection laser system, and (right) the generation laser system of the high frequency (HF) measurement system.

The sample surface displacement as a function of time is recorded by the detection system in what's known as an A-scan. A B-scan is a series of A-scans performed as a function of another parameter, such as a sweep across the sample surface. Some of the steps involved in the analysis going from a single measurement (A-scan) to a scan along the sample (B-scan), with consecutive temporal bandpass filtering and finally spatial smoothing, are shown in Figure 5 below.

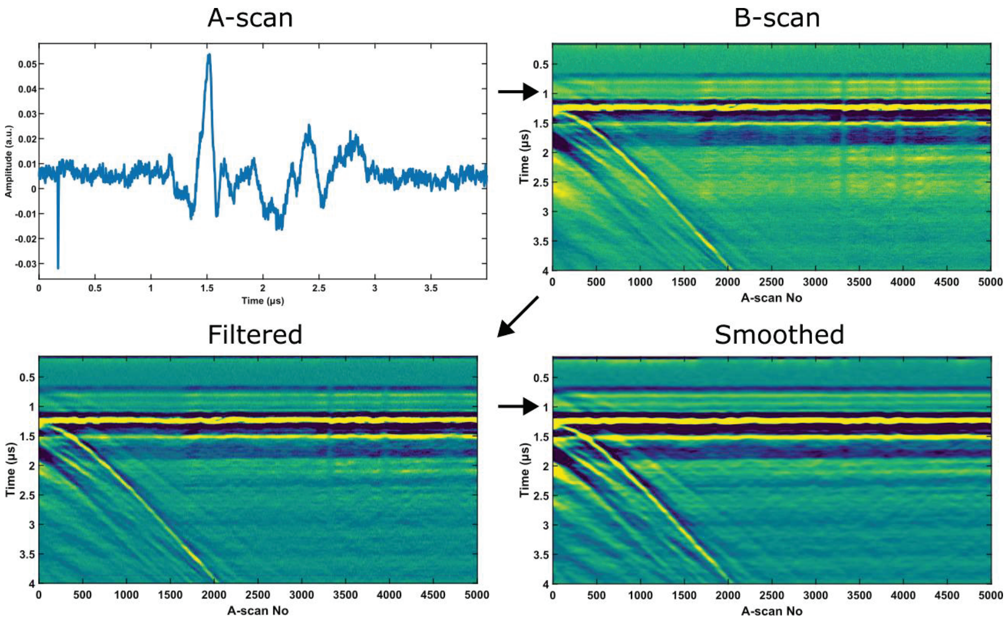

Figure 5: The data analysis steps involved in a typical LUS measurement: an A-scan showing displacement amplitude as a function of time, a B-scan collecting a number of A-scans, the B-scan with an applied 1-20 MHz bandpass filter, and with 11 measurements and 34 ns moving averages in the X and Y directions.

5. Objective

As stated in the application, the main goal of this pre-study was to provide a proof-of-concept and framework for later implementation of LUS technology in the production of EV batteries, as preparation for a possible full-scale research project.

The readiness level of the LUS implementation framework did not reach the level expected at the time of application. This is mainly due to the analysis of the LUS data being more challenging than expected for weld samples with induced porosity or surface defects. Since finding these features is critical for the utilization of this technique in production, a larger-scale project may be needed in order to acquire the amount of non-destructive and destructive data needed to make production decisions based on LUS measurements.

6. Results and deliverables

The application specified five work packages, each with a set of deliverables. The results of the deliverables are described below.

6.1 Requirements, criteria and evaluation methods in comparison to LUS

To be useful in a production environment, a LUS measurement system must reduce the rate of faults and/or the need for destructive or time-consuming testing enough that the cost and time savings exceed the cost of the system and time overhead in using it in production.

6.2 Sample selection and take-out

Volvo samples

Test samples were produced using base materials representative of busbars and terminals. The initial welding process employed a standard parameter set as a baseline. Subsequently, parameters were deliberately adjusted beyond the defined process window to induce controlled defects such as porosity and spatter. These intentional variations were introduced to evaluate whether Laser Ultrasound (LUS) technology could reliably detect such defects, thereby assessing its potential as a quality assurance method for laser welding applications.

Scania samples

In order to intentionally influence the size and distribution of the imperfections, it was decided to alter the line energy of the weld. It is well understood that changing the heat input during the remote laser beam welding process influences the stability of the weld, thus influencing the entrapment of imperfections such as environmental gases as pores, the recapture of melt material with insufficient momentum to escape as spatter, and with sufficient cooling rates, surface breaking pores[24]. Using aluminium, where oxides are a given, in an overlap configuration gives the conditions where the oxide can induce a porosity in the material with the correct parameter settings. It can also influence the turbulence and spatter of the weld pool. These manufactured defects can then be observed using LUS.

6.3 Set-up for evaluation of joints with LUS

The first step of the LUS measurements was to create two artificial pieces by electric discharge machining, as shown in in the figure below. The “varying width” sample presents two layers joined by a long “weld” whose width varies from 0-2 mm. The “varying thickness” sample has a constant 1.5 mm width for the weld but with the top layer thickness varying from 0.8 to 2 mm.

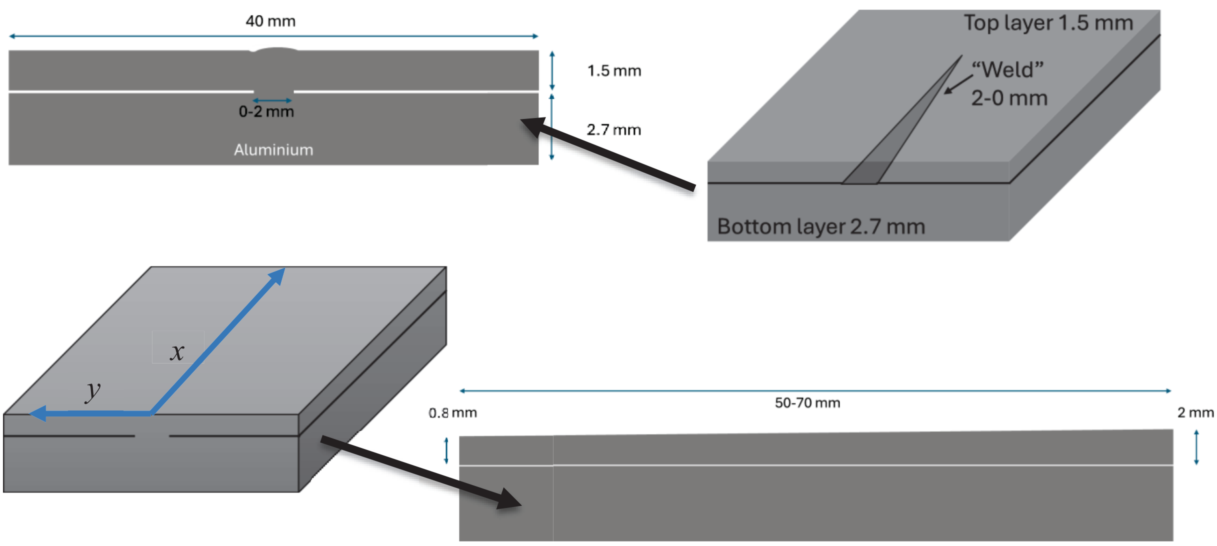

Figure 6: The artificial weld pieces: (top) the “varying width” sample; (bottom) the “varying thickness” sample. The x and y dimensions discussed below are shown on the varying thickness sample.

The artificial samples as well as the welded samples were mounted on an XY translation stage to enable scanning over the sample. This setup is shown for a welded sample in Figure 7 below, where an additional clamp was mounted on top of the stage in order to keep the surface under study straight.

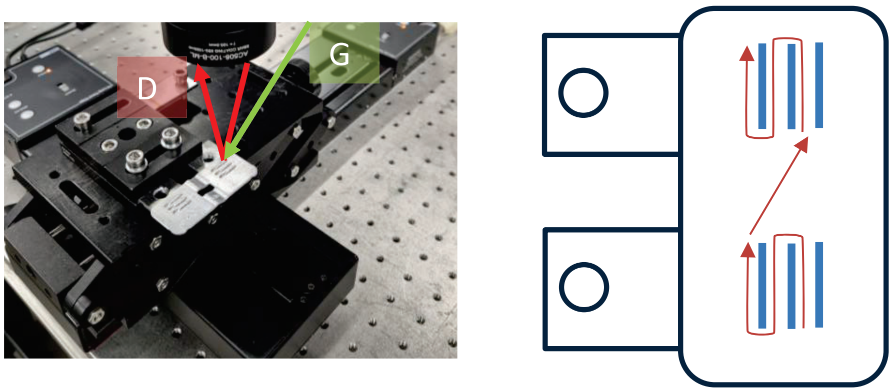

Figure 7: Setup for measurement on welded battery tabs. (left) the setup showing the generation laser G and detection laser D; (right) the scan performed on each sample, the red lines showing the position of the detection laser.

The high repetition rate of the high frequency laser system enables scanning parameters such as the position of the generation laser spot with the help of Galvano mirrors. The experiments described varied GY, the y position of generation, which can also be described in terms of the generation-detection distance GD, with y defined as in Figure 6.

A typical measurement with varying GD consists in shifting to a new position with each shot of the generation laser with the help of an arbitrary function generator (AFG). In the following data analysis, one selects every nth point, where n is the number of different generation positions.

6.4 LUS measurements and data analysis

Artificial samples

LUS measurements were performed on the artificial samples shown in more detail under the previous deliverable. The x and y dimensions discussed below are shown in the lower part of Figure 6.

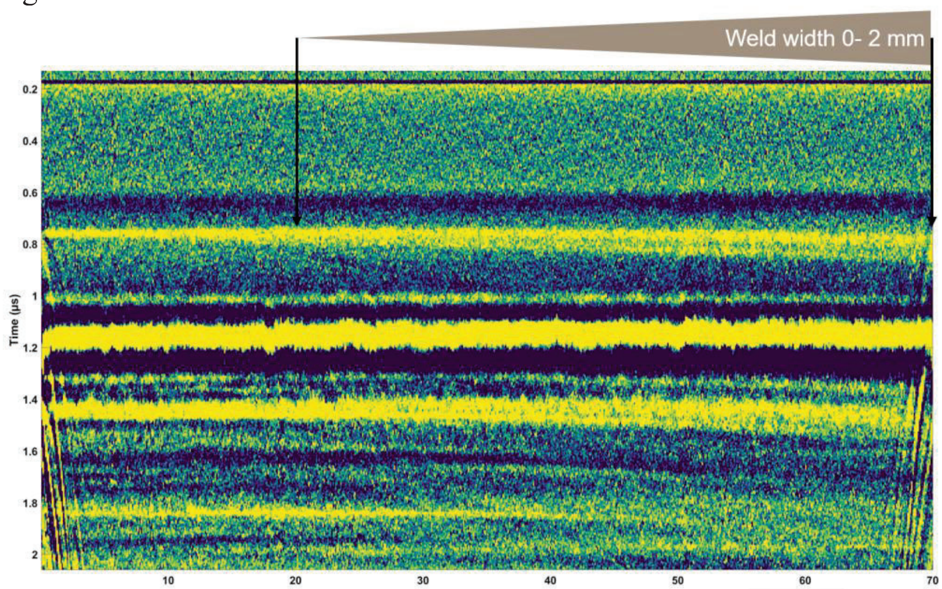

Figure 8: Raw B-Scan along the x-coordinate in mm for the varying width sample, with the approximate "weld" width shown on top.

Figure 8 above shows a B-scan in x spanning the entire length of the "varying width" sample. As can be seen, some features (such as the P-wave around 0.8 µs) vary more strongly with the weld width, showing that they probe the bulk more effectively. Others such as the surface skimming wave (around 0.65 µs) are insensitive to the weld width.

Figure 9 below shows six different B-scans at different generation positions where the detection laser is at $y = 0$ and the center of the weld is at around $y = 1.5$ mm. Compared to the raw signal, these scans have had a 40 ns smoothing and a 1-10 MHz band pass filter applied.

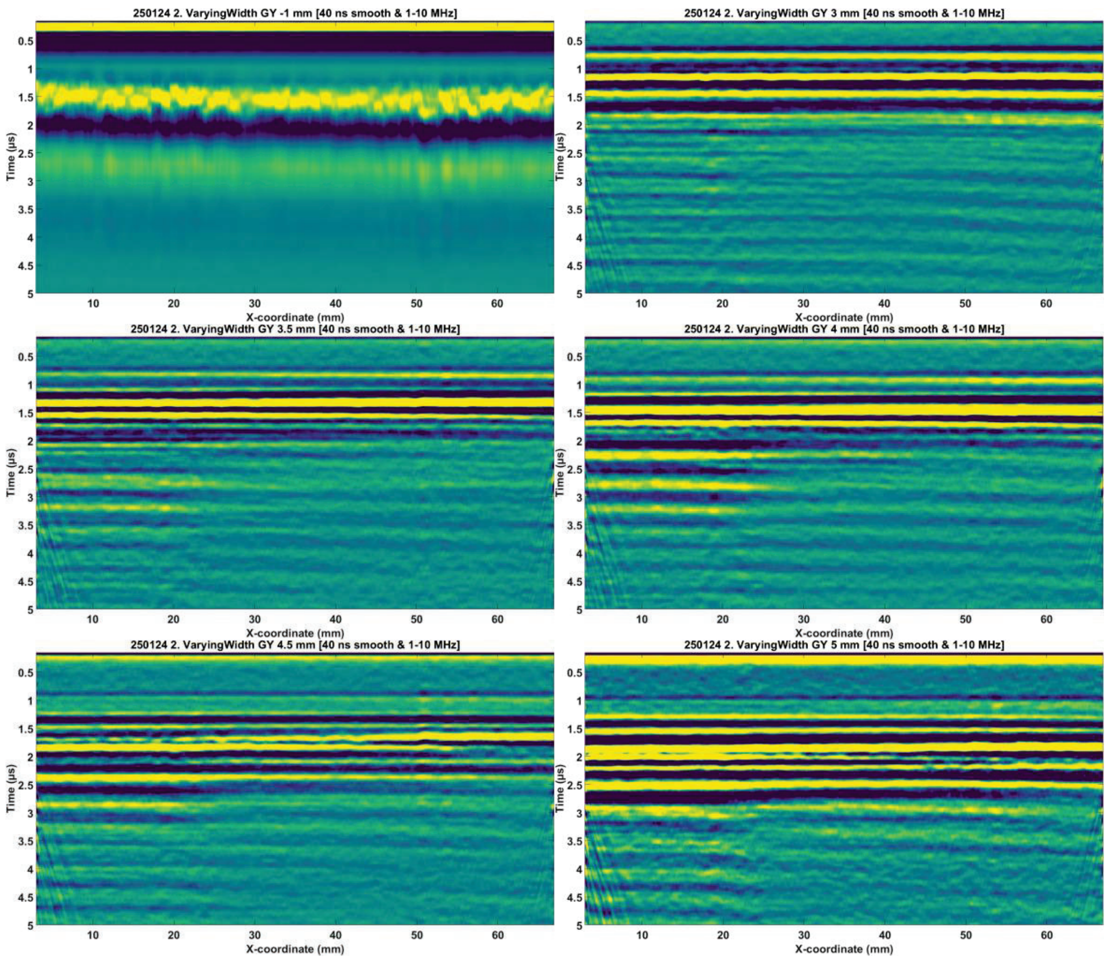

Figure 9: B-scans along the length of the varying width sample for six different generation positions: -1, 3, 3.5, 4, 4.5 and 5 mm, respectively.

From the scans above, several interesting features can be extracted and compared between the measurements at different GY positions. As the generation laser is at $y = 0$ and the GY values are positive, GD is equivalent and used in its place. Figure 10 below shows one of these features, the P-wave (pressure wave) velocity ratio for a given GD and the next one. Some linear fits are provided which do not individually correlate so well. However, the observation can be made that in this particular measurement the errors of $\frac{GD=3}{GD=3.5}$ (blue) and $\frac{GD=3.5}{GD=4}$ (orange) seem to cancel out, indicating that a combination of all measurements may lead to a better fit.

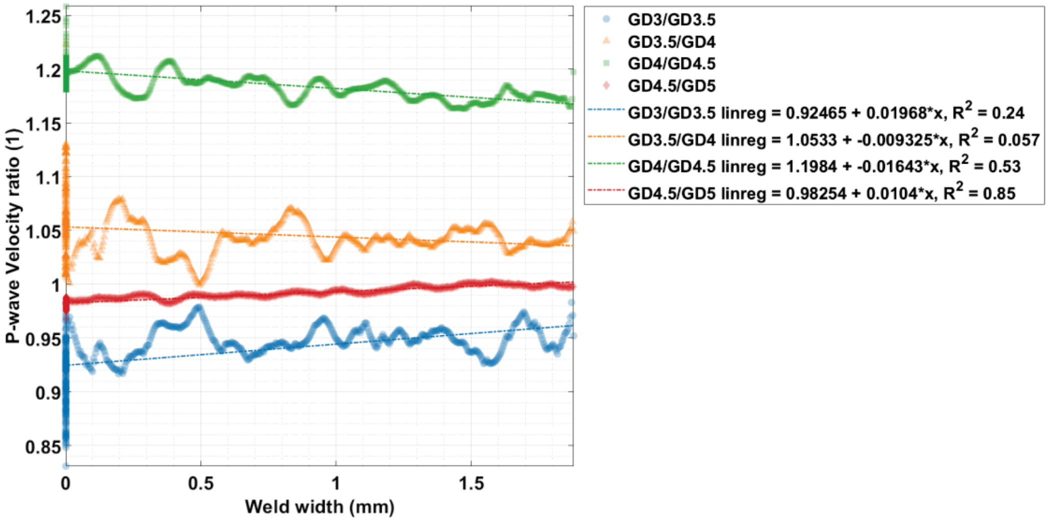

Figure 10: The velocity difference of the P-waves as found by subsequent GD values, along with linear fits. The data has been processed by a 21-point running average.

Combining all parameters, such as P-wave velocity ratio, time-of-flight offset of the Rayleigh wave, and the positive and negative amplitudes of the Rayleigh wave, leads to a more robust model as shown in the correlation plot below which compares the LUS measured weld width with the actual "weld width", a 1:1 line is added for visual aid.

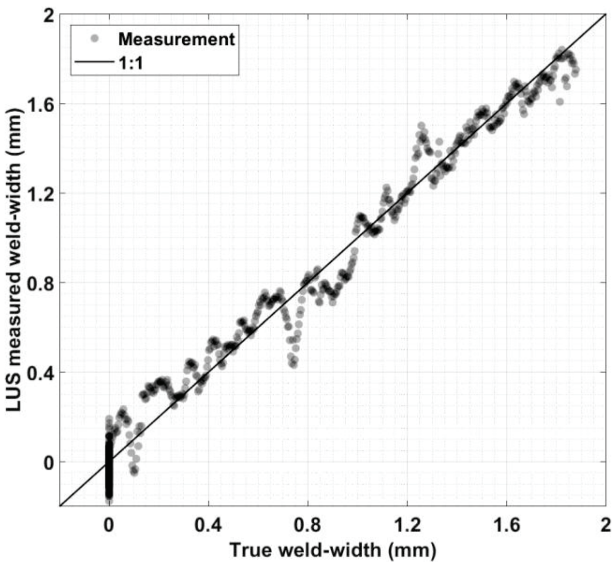

Figure 11: Correlation plot between the LUS measured weld width versus the true weld width of the calibration sample with varying weld width. The solid black line is a 1:1 proportional line to serve as a guide for the eye. The coefficient of determination for this correlation plot R^2 is 98 %.

The coefficient of determination for the combined fit is 98%, indicating a high degree of confidence in the model. Thus, this measurement may serve as a proof-of-concept indicating the ideal performance of a LUS-based weld monitoring system.

Welded samples

The Scania samples were cut into pieces consisting of two battery tabs and a connecting section of busbar, as shown in Figure 7. The generation laser was set to six different GY positions, shown relative to the weld in Figure 12 (right) below. As seen in the photo on the right, the sample was scanned around three welds in an "S" pattern, with the direction indicated by a blue pen mark. The final position of the detection laser can also be seen as a faint red dot to the left of the bottom weld.

Figure 12: (left) The generation and detection laser spots in relation to the weld; (right) the tracks created by scanning the sample, with the direction indicated by the blue pen mark. Different samples are shown in the two photos.

To simplify optical alignment and sorting of the data, each "half" sample of three welds was measured separately. Scans were performed in this fashion on 20 half samples. The results of one scan are shown in Figure 13, below. After applying a 1-30 MHz bandpass filter and separating the data by GY, the measurements were averaged by 20-point (40 ns) and 10-point (0.75 mm) running averages in the time and X dimensions, respectively.

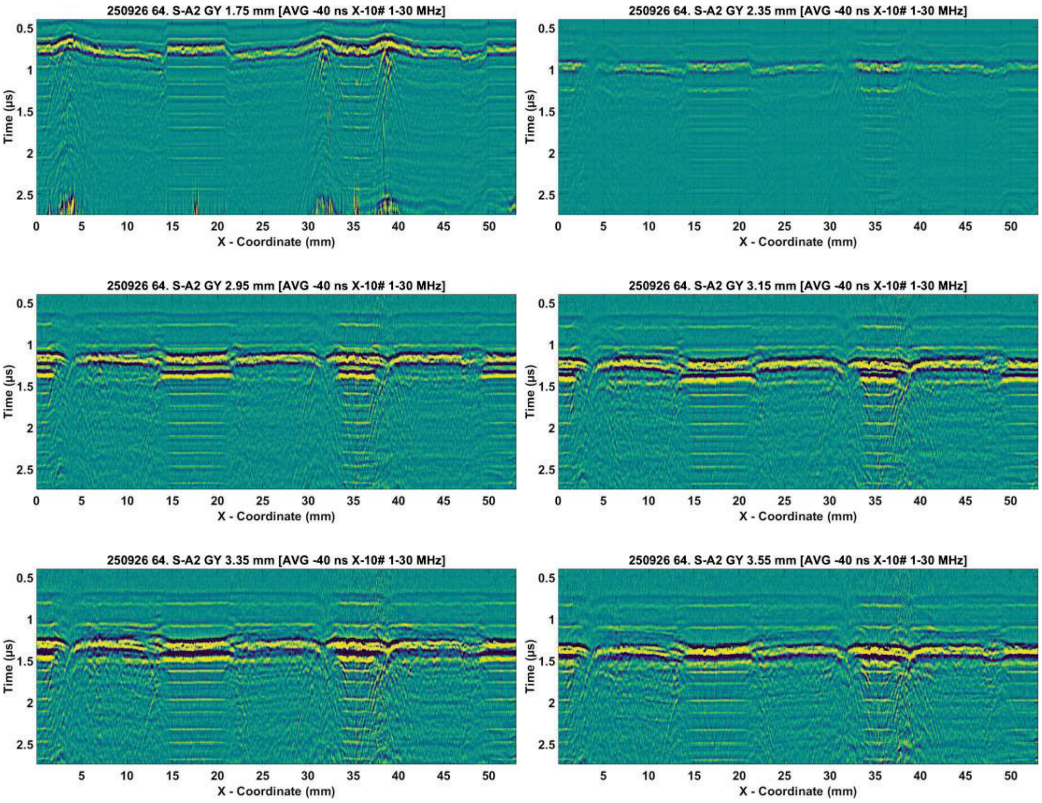

Figure 13: B-scans for Scania busbar sample A2, divided by GY position.

As seen in the figure, it is clear where there is no weld at all (around X = 0, 18, 36, and 54 mm in the X-scan), as many subsequent echoes of the top plate can be seen. However, it is more difficult to determine the quality of the welds. It is not fully determined what noisy features in the scan correspond to imperfections in the bulk of the weld (seen in Figure 19) as opposed to features affecting surface waves. More data (both LUS and destructive testing) is likely needed for a robust framework to determine the origin of these ultrasonic features.

For the Volvo samples, the "thin" samples were scanned as shown in Figure 14 below, for each group, with one measurement covering all groups on a given sample and split afterwards.

As seen in the inset of the figure and in a similar fashion to the Scania samples shown above, six GY values were used: the center of the weld (1), the edge of the weld (2), and four positions clear of the weld (3-6).

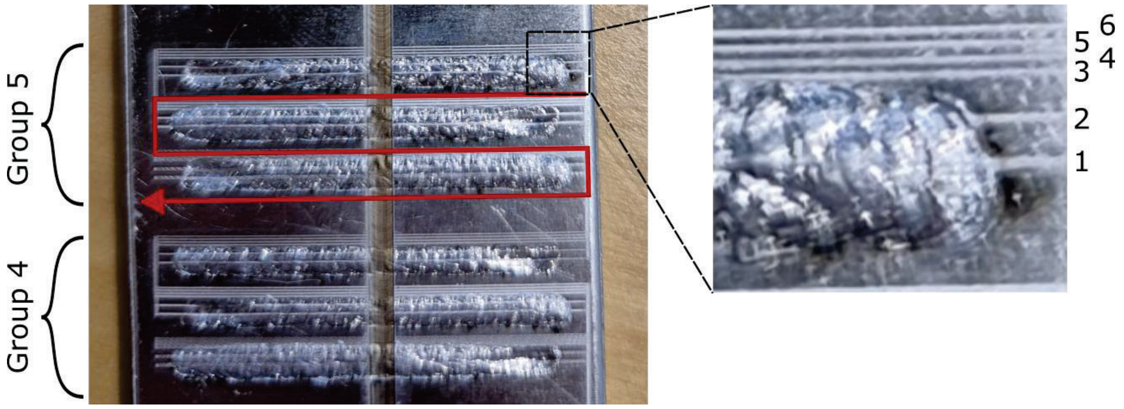

Figure 14: Sample and measurement geometry for Volvo samples, showing two groups out of six on a sample tab, with the red line showing the position of the detection laser. The inset highlights the tracks of the generation laser for six different GY.

The measurement points for each group were subsequently separated by GY, as shown in Figure 15 below.

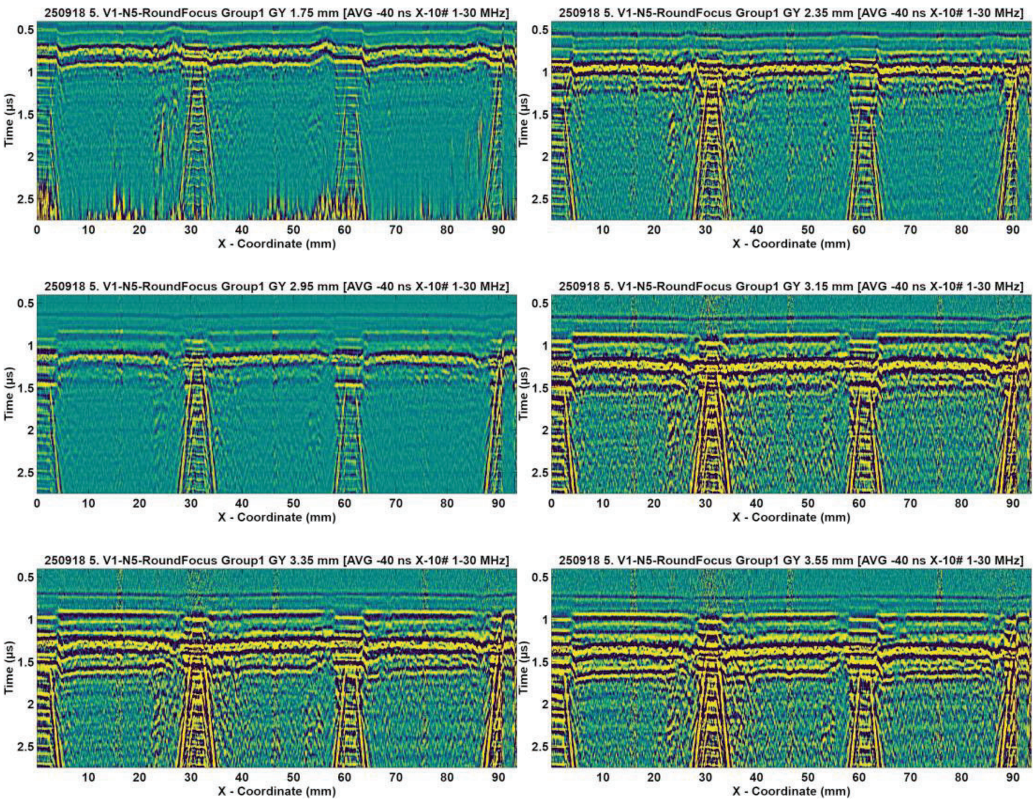

Figure 15: B-scans sweeping one group as shown in Figure 14, for the GY values shown in its inset. The regions of more activity around 0, 30, 60 and 90 mm correspond to measurements outside the welds.

The "thick" busbar samples could not be measured in the manner shown above. This is because the weld tracks overlapped on the surface, making the surface too rough to measure using the high frequency laser system. Instead, the high-power laser system was used to sweep across the welds, as previously demonstrated for resistance spot welding[15]. The result of a scan like this is shown in Figure 16, below.

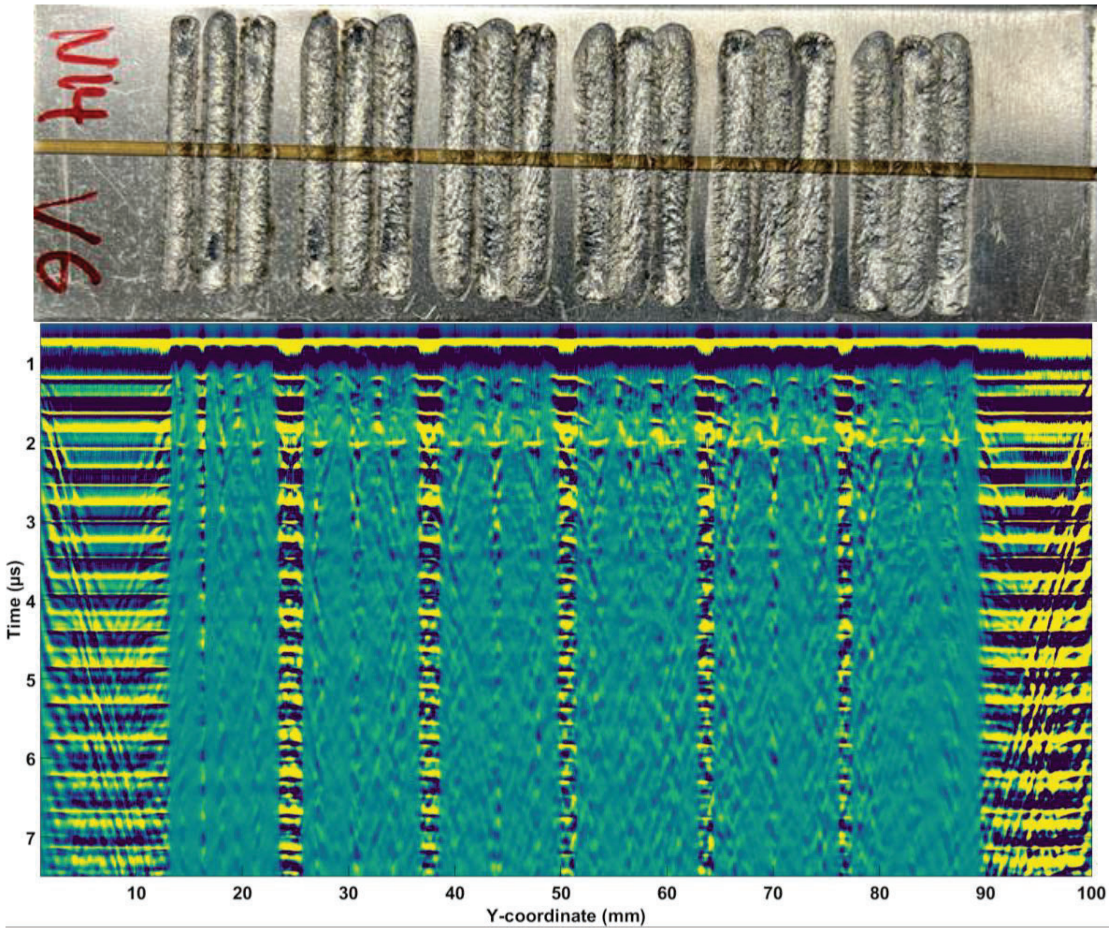

Figure 16: A "thick" busbar sampled scanned along the center line using the high-power laser system, with the corresponding B-scan (bottom).

In this figure, the characteristic "top piece" echoes are readily apparent between groups and at the edges of the sample; they can be seen for some points within groups but it's hard to make conclusive statements on the welds. It is also apparent that on the center of the weld the backwall echo of the joined top and bottom layer is visible at ~2 μs.

The B-scan above contains many noisy features in the weld region. These welds were intentionally made to contain more pores than usual by setting the laser parameters far from the optimal values, which is also evident in the microscope images taken of the cut surfaces shown in Figure 17.

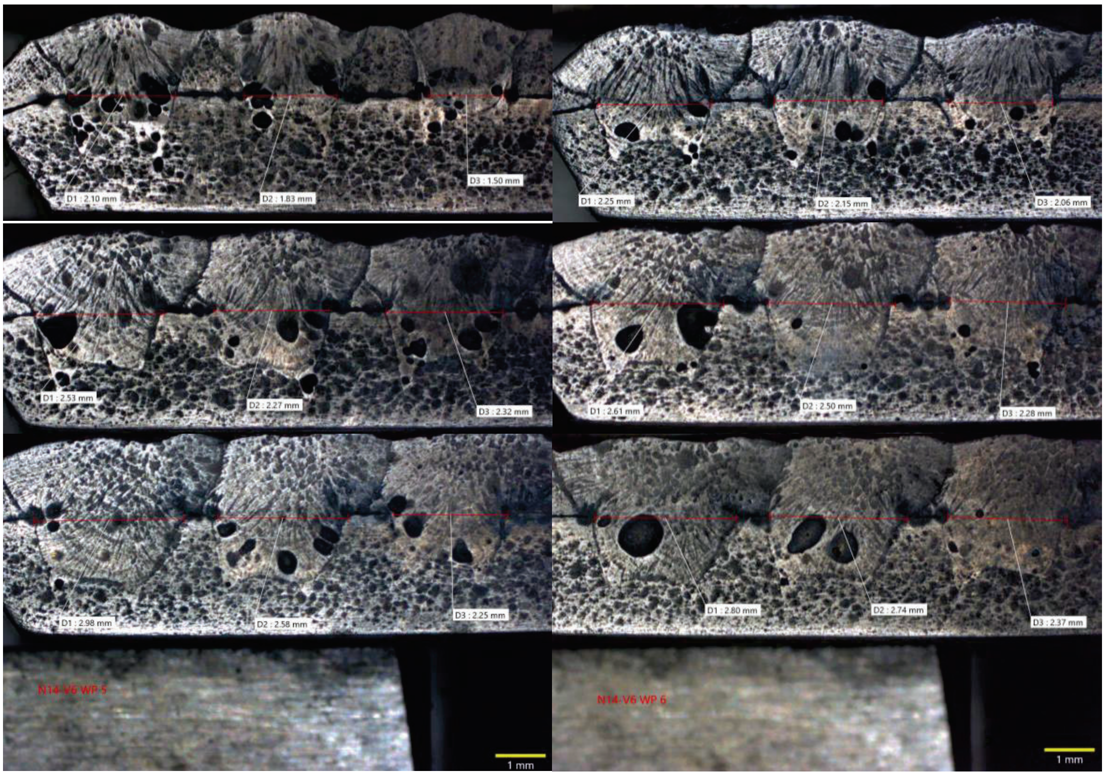

Figure 17: Micrographs of the cross section for the N14-V6 sample the 1 mm scalebar is visible in the bottom images and is the same for all images. From left to right and top to bottom, the images correspond to the groups of 3 welds in the previous figure from left to right.

The geometry of the welds also directs the ultrasound in slightly different directions which makes the analysis even more challenging.

6.5 Correlation plot showing measured weld area with LUS vs destructive / CT testing

A series of weld samples were made with laser parameters chosen to deliberately create porosity defects as shown in Figure 20 below. The sample was tested using computed tomography and subsequently by LUS, with the slices along the horizontal plane corresponding as closely as possible to the scanned X coordinate.

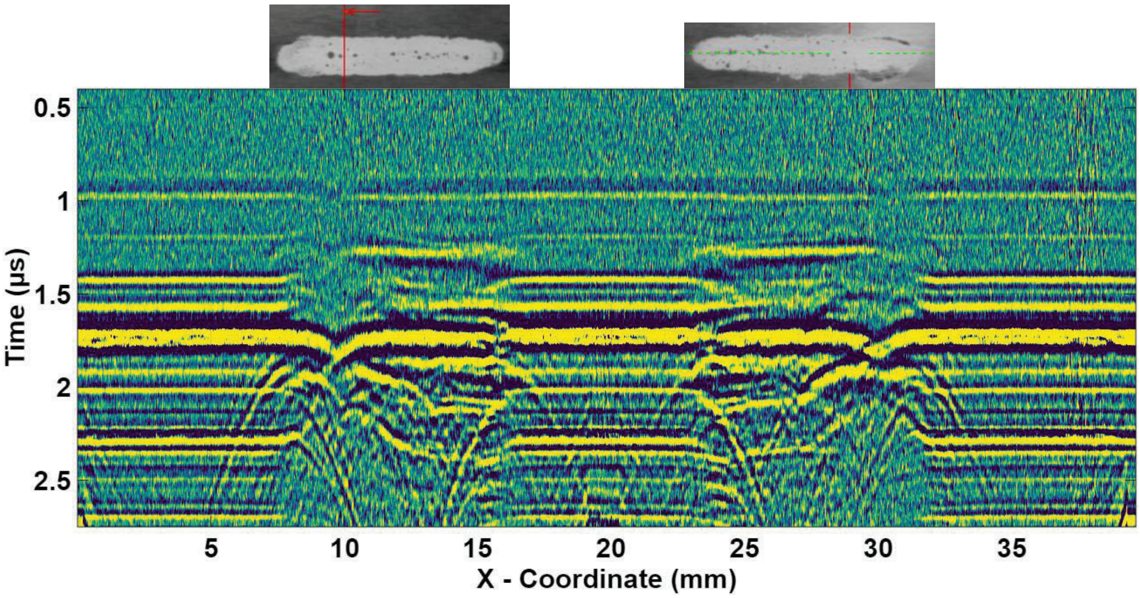

Figure 18: B-scan along two welds on a sample, with insets on top showing a horizontal slice through the CT measurement of the corresponding weld track.

As seen in the figure and discussed previously, at this stage of analysis it is not trivial to correlate features seen in the B-scan and the CT measurement. With more data, it should be possible that the influence of factors such as surface quality can be minimized in order to correlate the features more clearly.

6.6 Benchmarking LUS with conventional technique

Benchmarking of LUS measurements compared to other techniques is still ongoing and is expected to improve as more data becomes available. However, apart from CT of the whole battery case no other non-destructive method has been found that also allows for measuring the bulk properties of the weld with single sided access that has the potential to be implemented in an online setting in the production line.

6.7 Benchmarking with conventional destructive testing

In complement to CT scanning, which shows the presence of porosity at a slice level, a traditional metallographic sample was prepared using the Scania A2 sample, Figure 19.

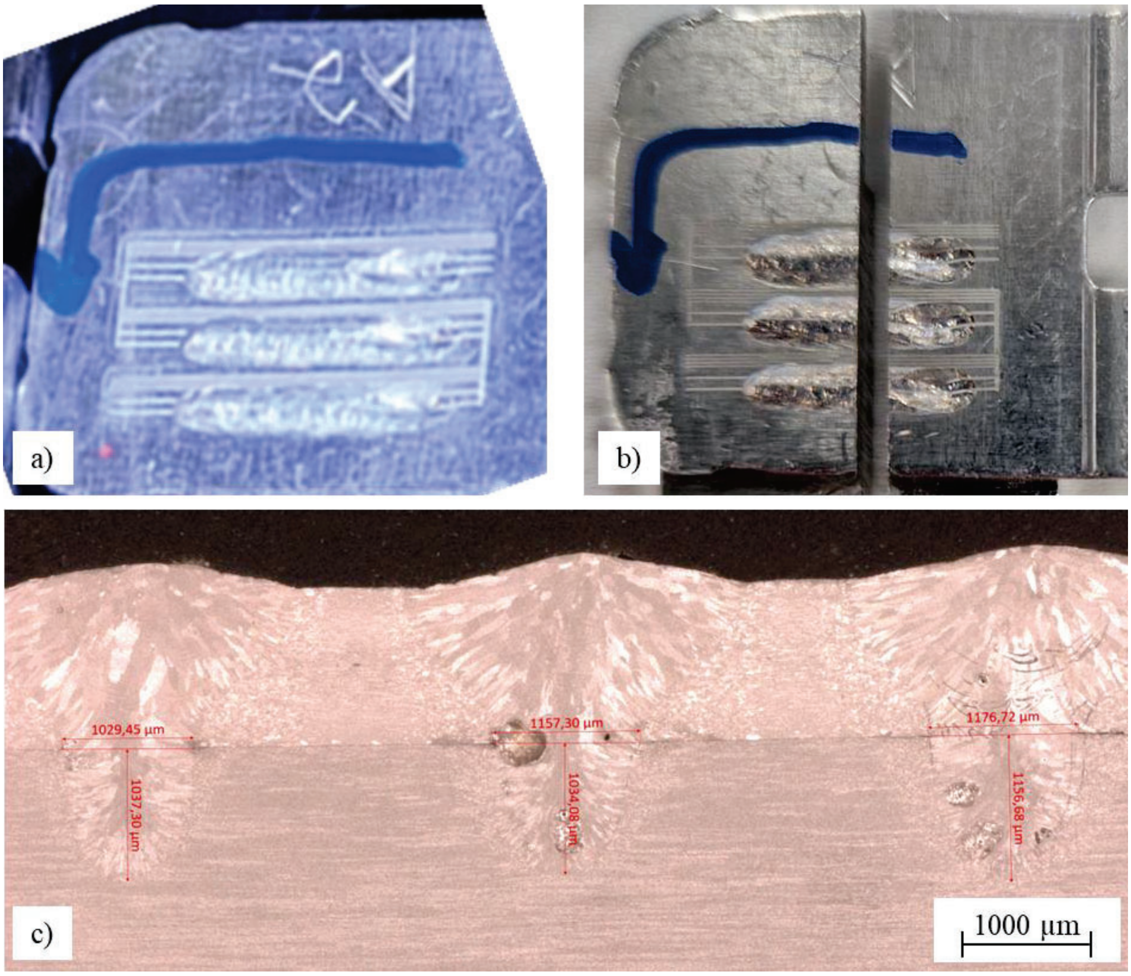

Figure 19: a) Scania sample as delivered, b) sample A2 after machine cutting, and c) cross-section of research parameter sample A2 showing large and small pores.

As noted in the CT scans, there is a distribution of pores both in terms of the size and location. In this particular weld parameter set, small nearly circular pores are seen while the larger pores have a noticeable surface texture. As previously discussed at Figure 13, it is currently a challenge to isolate the impact of the inherent weld surface quality from the bulk material, and here in Figure 19 it shows that at a slice level, the surface of the weld has a relatively smooth profile. This smooth profile cannot be seen for all of the pores in this weld cross-section, and thus could be the likely point of the noise in the signal collected by the LUS receiver.

As the measurement lines move away from the weld center-line, the deeper pores, like that of Figure 19c on the right hand side, could become “visible” to the wave propagation, with the wave reflections then being able to bounce off numerous pores and causing a distortion in the measurement.

To confirm this, further investigations would be needed where the surface of the weld is prepared in such a way to produce a relatively smooth surface such that the only reasonable signal disturbance comes from the internal porosity.

6.8 Measurements with other techniques

Thus far, measurements using other (nondestructive and feasibly in-line) techniques have not been performed yet; it is expected that the improved LUS measurements can give an insight into which other techniques (and modes of measurement) would prove most useful.

6.9 Literature study on implementation and benchmarking

Given the growth of the battery production field, battery inspection has received quite some attention in literature. An overview of the literature relating to the measurements shown in this report and discussed in terms of future implementation can be found in the References section.

6.10 A first framework for implementation and requirement specification of hardware and measurement methodology

A framework for future measurements is under preparation for distribution among the project partners.

6.11 Set up project website for communication

A common project area was set up within Swerim’s IT infrastructure to share results and data within the project.

6.12 Technical reports and dissemination

Given the limited scope of this pre-study, this public report serves as the main dissemination of the work, outside the project group itself.

7. Dissemination and publications

7.1 Dissemination

How are the project results planned to be used and disseminated?	Mark with X	Comment
Increase knowledge in the field		
Be passed on to other advanced technological development projects	X	The project group's intention is that the results attained in this project will serve as input into a future full scale project application. In which LUS is investigated in more detail as a method for non-destructive battery weld examination and bring the technology readiness level up closer towards industry implementation.
Be passed on to product development projects		
Introduced on the market		
Used in investigations / regulatory / licensing / political decisions		

7.2 Publications

The work has been presented in part within the member companies. Apart from this public report, no other publications are planned outside the project group.

8. Conclusions and future research

There is now an increased understanding of the challenges involved in introducing LUS measurements as an in-line inspection technique for battery welding. Mitigation of the challenges is outside the scope of this work, but some clear starting points have been defined for future projects.

8.1 Need for large data sets

In the course of measuring and analyzing the welded samples, it became apparent that large amounts of data would be needed to effectively determine bulk effects in the tested samples and separate them from noise caused by surface features. A larger data set would also be necessary for more advanced data analysis methods such as developing machine learning methods for determining the weld quality.

8.2 Alternate ultrasound geometries

Determining whether features in the LUS scan originated inside the weld emerged as a challenge when measuring actual welded samples. One way to achieve a stronger signal from the weld specifically could be to alter the geometry of generation and detection, as shown in the figure below. In this setup, the ultrasound pulse is generated in the lower piece and can only propagate to the upper piece (where detection takes place) where a successful weld has coupled the two sections. This has previously been attempted for studying welds to individual foil sheets within a battery cell[14].

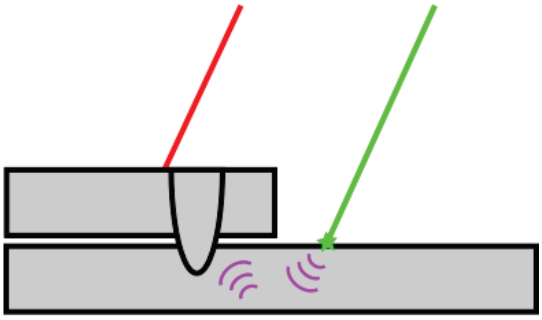

Figure 20: Monitoring ultrasound waves (purple) travelling through the weld. The generation laser (green) hits the lower piece, and the detection laser (red) scans the upper piece.

Another method of more directly addressing the weld could be to generate and detect the ultrasound from opposite sides of the workpiece but this clearly reduces the “in-line” utility of the technique as both sides of the workpiece must be accessible.

9. Participating parties and contact persons

Swerim AB: Mikael Malmström, Pia Borg, Hampus Wikmark Kreuger
Scania CV AB: David Löveborn, Mattias Olsson, Stephanie Robertson, Linda Graaf Söderberg
Volvo Personvagnar AB: Yves van den Stock

10. References

(1) Zwicker, M. F. R.; Moghadam, M.; Zhang, W.; Nielsen, C. V. Automotive Battery Pack Manufacturing – a Review of Battery to Tab Joining. *J. Adv. Join. Process.* **2020**, *1*, 100017. https://doi.org/10.1016/j.jajp.2020.100017.

(2) Rinker, T. J.; McGovern, M. E.; Brown, T.; Wang, H. Thermographic Detectability of Porosity in Multi-Layered Bare and Anodized Aluminum Laser Welds. *Procedia Manuf.* **2020**, *48*, 165–171. https://doi.org/10.1016/j.promfg.2020.05.034.

(3) Malmström, M.; Jansson, A.; Hutchinson, B.; Lönnqvist, J.; Gillgren, L.; Bäcke, L.; Sollander, H.; Bärwald, M.; Hochhard, S.; Lundin, P. Laser-Ultrasound-Based Grain Size Gauge for the Hot Strip Mill. *Appl. Sci.* **2022**, *12* (19), 10048. https://doi.org/10.3390/app121910048.

(4) Hoppe, D.; Haschke, T.; Sprock, A.; Hassel, C.; Hafer, J.; Bäcke, L.; Thorberg, J.-E.; Jonsson, C.; Malmström, M.; Kneisel, F.; Bärwald, M. New Insights into the Online LUS Grain Size Measurements; ESTAD 2025; Associazione Italiana di Metallurgia: Verona; pp 227–234.

(5) Lin, M.; Roy, S.; Militzer, M. In Situ Measurement of Austenite Grain Growth and Recrystallization Using Laser Ultrasonics. *J. Phys. Conf. Ser.* **2023**, *2635* (1), 012039. https://doi.org/10.1088/1742-6596/2635/1/012039.

(6) Malmström, M.; Bäcke, L.; Magnusson, H.; Lönnqvist, J.; Hutchinson, B. Investigation of Dynamic Recrystallisation of Steel During Hot Compression Using Gleeble and Laser-Ultrasonics (GLUS). *Metall. Mater. Trans. A* **2025**. https://doi.org/10.1007/s11661-025-07834-0.

(7) Hutchinson, B.; Malmström, M.; Jansson, A.; Lönnqvist, J. An Experimental Study of Elasticity in Polycrystalline Iron. *Phys. Status Solidi B* **2025**, 2500044. https://doi.org/10.1002/pssb.202500044.

(8) Keyvani, M. Laser Ultrasonic Investigations of Recrystallization and Grain Growth in Cubic Metals, University of British Columbia, 2018. https://doi.org/10.14288/1.0365293.

(9) Garcin, T.; Schmitt, J. H.; Militzer, M. In-Situ Laser Ultrasonic Grain Size Measurement in Superalloy INCONEL 718. *J. Alloys Compd.* **2016**, *670*, 329–336. https://doi.org/10.1016/j.jallcom.2016.01.222.

(10) Hayashi, N.; Rodrigues, M. C. M.; Militzer, M. In-Situ Laser Ultrasonics Measurements of Ferrite Formation during Stepped Cooling of A 0.1C-2Mn Dual Phase Steel. *ISIJ Int.* **2024**, *64* (5), 817–825. https://doi.org/10.2355/isijinternational.ISIJINT-2023-331.

(11) Lindgren, E.; Malmström, M.; Janiak, P.; Wirdelius, H.; Sandström, U.; Stenberg, K. *Avancerad Kvalitetssäkring Av Limmade Och Svetsade Förband (QUALITY II)*; 2014–03949; p 49. https://www.vinnova.se/globalassets/mikrosajter/ffi/dokument/slutrapporter-ffi/hallbar-produktion-rapporter/sr2014-03949_quality2_sv.pdf.

(12) Grasley, A.; Guo, H.; Hiraiwa, M.; Nadeau, A.; Stautz, M. Laser Ultrasonic Inspection of Mash Seam Welds in a Steel Mill. In *AISTech 2023 Proceedings*; AIST, 2023; pp 1616–1624. https://doi.org/10.33313/387/179.

(13) Gattani, V. S.; McGovern, M. E.; Bruder, D.; Rinker, T. J. Laser Ultrasound Wave Propagation in Multi-Layer Laser-Welded Joints and Implications on Substrate Interface Defect Detection; Livonia, MI, 2021.
(14) Huemiller, E.; McGovern, M.; Du, X.; Salvador, J.; Wagner, S.; Collin, W. Industrial EV Battery Performance Evaluation: A Review From the Instrumentation Perspective. *IEEE Open J. Instrum. Meas.* **2025**, *4*, 1–13. https://doi.org/10.1109/OJIM.2025.3544347.
(15) Jansson, A.; Malmström, M.; Lundin, P. Laser Ultrasonics for Quality Control of Resistance Spot Welding, 2022. https://lus4metals.sciencesconf.org/data/program/Jansson_397942.pdf (accessed 2025-11-12).
(16) Klein, M. B.; Pouet, B.; Kercel, S.; Kisner, R. In-Process Detection of Weld Defects Using Laser Ultrasonics. In *ICALEO 2001: Proceedings of the Laser Materials Processing Conference and Laser Microfabrication Conference*; Laser Institute of America: Jacksonville, Florida, USA, 2001; pp 1118–1125. https://doi.org/10.2351/1.5059771.
(17) Miller, M.; Mi, B.; Kita, A.; Ume, I. C. Development of Automated Real-Time Data Acquisition System for Robotic Weld Quality Monitoring. *Mechatronics* **2002**, *12* (9–10), 1259–1269. https://doi.org/10.1016/S0957-4158(02)00028-4.
(18) Blecher, J. J.; Galbraith, C. M.; Van Vlack, C.; Palmer, T. A.; Fraser, J. M.; Webster, P. J. L.; DebRoy, T. Real Time Monitoring of Laser Beam Welding Keyhole Depth by Laser Interferometry. *Sci. Technol. Weld. Join.* **2014**, *19* (7), 560–564. https://doi.org/10.1179/1362171814Y.0000000225.
(19) Dupriez, N. D. Smart Monitoring of Battery Welding Processes: Sensor Systems for Laser Welding Applications along the Battery Production Chain: From Cell to Package. *PhotonicsViews* **2021**, *18* (5), 46–50. https://doi.org/10.1002/phvs.202100045.
(20) Webster, P. J. L.; Wright, L. G.; Ji, Y.; Galbraith, C. M.; Kinross, A. W.; Van Vlack, C.; Fraser, J. M. Automatic Laser Welding and Milling with in Situ Inline Coherent Imaging. *Opt. Lett.* **2014**, *39* (21), 6217. https://doi.org/10.1364/OL.39.006217.
(21) Stavropoulos, P.; Bikas, H.; Sabatakakis, K.; Theoharatos, C.; Grossi, S. Quality Assurance of Battery Laser Welding: A Data-Driven Approach. *Procedia CIRP* **2022**, *111*, 784–789. https://doi.org/10.1016/j.procir.2022.08.129.
(22) McGovern, M. E.; Rinker, T. J.; Sekol, R. C. Assessment of Ultrasonic Welds Using Pulsed Infrared Thermography. *J. Nondestruct. Eval. Diagn. Progn. Eng. Syst.* **2019**, *2* (1), 011009-011009–9. https://doi.org/10.1115/1.4042260.
(23) Passini, A.; Oliveira, A. C. D.; Riva, R.; Travessa, D. N.; Cardoso, K. R. Ultrasonic Inspection of AA6013 Laser Welded Joints. *Mater. Res.* **2011**, *14* (3), 417–422. https://doi.org/10.1590/S1516-14392011005000057.
(24) Robertson, S. M.; Kaplan, A. F. H.; Frostevarg, J. Material Ejection Attempts during Laser Keyhole Welding. *J. Manuf. Process.* **2021**, *67*, 91–100. https://doi.org/10.1016/j.jmapro.2021.04.052.